PHYSICAL REVIEW E **84**, 031125 (2011)

Multiterm solution of a generalized Boltzmann kinetic equation for electron and positron transport in structured and soft condensed matter

R. D. White[*] and R. E. Robson

ARC Centre for Antimatter-Matter Studies, School of Engineering and Physical Sciences, James Cook University, Townsville 4810, Australia

(Received 9 June 2011; revised manuscript received 4 August 2011; published 23 September 2011)

In this paper, we generalize the semiclassical Boltzmann kinetic equation for dilute gases to consider highly nonequilibrium electrons and positrons in soft condensed matter, accounting rigorously for all types of interactions, including positronium formation, and allowing for both coherent and incoherent scattering processes. The limitations inherent in the seminal paper of Cohen and Lekner [M. H. Cohen and J. Lekner, Phys. Rev. **158**, 305 (1967); Y. Sakai, J. Phys. D **40**, R441 (2007)] are avoided by solving the kinetic equation using a "multiterm" spherical harmonic representation of the velocity distribution function, as well as formulating a necessarily nonperturbative treatment of nonconservative collisional processes such as positronium formation. Numerical calculations of transport properties are carried out for a Percus-Yevick model of a hard-sphere system, and for positrons in liquid argon. New phenomena are predicted, including structure-induced negative conductivity and anisotropic diffusion.

DOI: 10.1103/PhysRevE.84.031125 PACS number(s): 05.20.Dd, 34.80.Uv, 36.10.Dr

I. INTRODUCTION

New frontiers in science and technology have generated a fresh wave of interest in understanding the fundamental physics of electron and positron transport processes in various structured and soft condensed materials. For electrons, these applications range from liquid-based particle detecting time projection chambers [1] to organic materials and solar cells [2] and to understanding radiation damage in biological matter [3,4]. For positron-based systems, the emission of back-to-back gamma rays resulting from annihilation of a positron and an electron is an established investigative tool in a number of fields of science and technology, ranging from fundamental atomic and molecular physics, particle and astrophysics, to diagnostics in biological and material sciences, e.g., positron emission tomography (PET) [5] and positron annihilation lifetimes spectroscopy (PALS) [6], respectively. The understanding and optimization of these technologies requires a fundamental understanding of the underpinning physical processes involved, including accurate knowledge of the input electron and positron scattering cross sections, material structure, and transport theories.

While much is accurately known for electron interaction processes (see, e.g., reviews [7–9]), information of equivalent accuracy for positrons has only recently become available through advances in beam scattering techniques using improved positron trapping systems (e.g., Penning-Malmberg-Surko traps) to produce high resolution positron beams [10,11]. The availability of new accurate complete sets of positron interaction cross sections has facilitated new theoretical investigations of positron transport. The effect of positronium (Ps) formation on transport processes is of special interest, with striking new phenomena such as Ps-induced negative differential conductivity in gases [12,13] and liquids [14] being reported. Electron and positron transport in dense gaseous and liquid systems has long been studied through kinetic theory, by solving the classical Boltzmann equation as modified by Cohen and Lekner [15,16], to take into account the effects of coherent scattering from background material and associated multiple scattering effects. For a review of the status of electron transport in liquid and dense gaseous systems, the reader is referred to the recent review of Sakai [16] and other prominent authors in the field [17,18]. However, Cohen and Lekner's kinetic equation is derived and utilized explicitly within the context of the "two-term" representation of the electron velocity distribution function, in which the spherical harmonic representation in velocity space is limited to two terms and is thus limited to situations of quasi-isotropy. Such situations are generally the exception rather than the rule in gaseous electronics [19], and there is every reason to believe that this is also the case for electrons and positrons in condensed matter. In addition, the two-term formulation suppresses angular effects arising from the static structure function $S(\boldsymbol{K})$ used to include the effects of material structure in the transport theory. In numerical solutions of the Boltzmann equation, spherical harmonic expansions must be truncated to finite size by imposing some upper limit $l_{\max}$ on the summation, but this must be regarded as a free parameter, to be incremented until the desired accuracy is achieved. In gaseous electronics, it is not unusual to find that "multiterm" representations with $l_{\max} \geqslant 5$ are required to achieve the desired result. For electrons or positrons in condensed matter, $S(\boldsymbol{K})$ introduces a further angular dependence, the full effects of which are impossible to ascertain within the narrow confines of the Cohen-Lekner quasi-isotropy formalism. For that reason, it has been necessary to reformulate a more general Boltzmann equation for light particles in structured matter [14].

In this paper, we further develop the recent multiterm formalism for electrons and positrons in structured matter [14]. This is followed by numerical investigations, first for a benchmark model system, and then for liquid argon using a comprehensive set of positron impact cross sections [12]. We are particularly interested in the effects of the material structure, and find interesting phenomena, including structure-induced negative differential conductivity and

---

[*] ronald.white@jcu.edu.au

structure-induced anisotropic diffusion. Another theoretical study of positrons in liquid Ar [20] confined their attention to thermalization times, using a two-term solution of the spatially homogeneous Boltzmann equation. Transport coefficients such as drift velocity and diffusion coefficients were not considered by [20] and, furthermore, *Ps* formation was treated as a weak perturbation, something which appears of questionable validity given the very large *Ps* formation cross section [12]. In this paper, we calculate a full set of measurable transport coefficients, and treat positronium formation in a rigorous, nonperturbative way.

II. THEORY

A. The kinetic equation and its multiterm solution in the hydrodynamic regime

The governing equation, describing a swarm of free light charged particles moving through materials (condensed or gas phase) driven out of equilibrium through the application of an electric field $\boldsymbol{E}$, is the Boltzmann equation for the phase space distribution function $f(\boldsymbol{r},\boldsymbol{c},t)$ [15,16]:

$$\frac{\partial f}{\partial t} + \boldsymbol{c}\cdot\nabla f + \frac{q\boldsymbol{E}}{m}\cdot\frac{\partial f}{\partial \boldsymbol{c}} = -J(f). \tag{1}$$

Here $\boldsymbol{r}$ and $\boldsymbol{c}$ denote, respectively, the position and velocity coordinates in phase space, while q and m are the charge and mass of the particle, respectively. In general, the rate of change of f due to interactions with the background material is described by the collision operator,

$$J(f) = J_{\text{coherent}} + J_{\text{incoherent}} = J_{\text{elast}} + J_{\text{inel}} + J_{Ps} + \cdots, \tag{2}$$

which accounts for all possible scattering processes, coherent and incoherent, through appropriate interaction cross sections and the structure function of the medium. The form of this collision operator varies depending on the material under investigation, and the details of the collision operators for coherent and incoherent scattering processes are left to Sec. II B.

To solve the Boltzmann Eq. (1) in the hydrodynamic regime, we make a series of representations of the various dependencies in $f(\boldsymbol{r},\boldsymbol{c},t)$. The angular dependence of the phase-space distribution function in velocity space can be represented in terms of an expansion in spherical harmonics:

$$f(\boldsymbol{r},\boldsymbol{c},t) = \sum_{l=0}^{\infty}\sum_{m=-l}^{l} f_m^{(l)}(\boldsymbol{r},c,t)Y_m^{[l]}(\hat{\boldsymbol{c}}), \tag{3}$$

where $Y_m^{[l]}(\hat{\boldsymbol{c}})$ are spherical harmonics and $\hat{\boldsymbol{c}}$ denotes the angles of $\boldsymbol{c}$. While it is traditional (in the two-term approximation) to set the upper bound of the l summation to 1 and set $m = 0$ (i.e., a Legendre polynomial expansion), we do not make such a restrictive assumption in this theory.

Various numerical techniques are applicable to represent the speed and energy space [21,22]. In this paper, we employ an expansion in terms of generalized Sonine (generalized Laguerre) $R_{\nu l}(\alpha c)$ polynomials [23],

$$f_m^{(l)}(\boldsymbol{r},c,t) = w(\alpha,c)\sum_{\nu=0}^{\infty} F_\alpha(\nu l m;\boldsymbol{r},t)R_{\nu l}(\alpha c), \tag{4}$$

which are orthonormal with respect to a Maxwellian weight function $w(\alpha,c) = (\frac{\alpha^2}{2\pi})^{3/2}\exp\{\frac{-\alpha^2c^2}{2}\}$, where $\alpha^2 = \frac{m}{kT_b}$. In the modern approach, one sets T_b to be the charged-particle temperature or an arbitrary basis temperature [24]. These are traditionally referred to as the "two-temperature theory" [24,25]. Combining (3) and (4) yields

$$f(\boldsymbol{r},\boldsymbol{c},t) = w(\alpha,c)\sum_{\nu=0}^{\infty}\sum_{l=0}^{\infty}\sum_{m=-l}^{l} F_\alpha(\nu l m;\boldsymbol{r},t)\phi_m^{[\nu l]}(\alpha\boldsymbol{c}), \tag{5}$$

where $\phi_m^{[\nu l]}(\alpha\boldsymbol{c}) = R_{\nu l}(\alpha c)Y_m^{[l]}(\hat{\boldsymbol{c}})$ are Burnett functions [25,26] which satisfy the following orthonormality relation:

$$\int w(\alpha,c)\phi_{m'}^{(\nu'l')}(\alpha\boldsymbol{c})\phi_m^{[\nu l]}(\alpha\boldsymbol{c})d\boldsymbol{c} = \delta_{\nu'\nu}\delta_{l'l}\delta_{m'm}. \tag{6}$$

In what follows, for brevity where appropriate, we will refer to equations in [25] with a prefix I.

Substituting (5) into (1), and utilizing the orthonormality of the basis functions, we obtain the following infinite set of partial differential equations for the moments $F_\alpha(\nu l m;\boldsymbol{r},t)$:

$$\begin{aligned}\frac{\partial F_\alpha(\nu l m)}{\partial t} &+ \sum_{\nu'=0}^{\infty}\sum_{l'=0}^{\infty}\sum_{m'=-l'}^{l'} \\ &\times\left[\langle \nu l m\|\boldsymbol{c}\cdot\nabla + \frac{q\boldsymbol{E}}{m}\cdot\frac{\partial}{\partial\boldsymbol{c}}\|\nu'l'm'\rangle\right]F_\alpha(\nu l m) \\ &= \sum_{\nu'=0}^{\infty}\sum_{l'=0}^{\infty}\sum_{m'=-l'}^{l'}\langle \nu l m\|J\|\nu'l'm'\rangle F_\alpha(\nu l m),\end{aligned} \tag{7}$$

where $\langle \nu l m\|\boldsymbol{c}\cdot\nabla + \frac{q\boldsymbol{E}}{m}\cdot\frac{\partial}{\partial\boldsymbol{c}}\|\nu'l'm'\rangle$ and $\langle \nu l m\|J\|\nu'l'm'\rangle$ are matrix elements, with the latter collision operator defined according to

$$\langle \nu l m\|J\|\nu'l'm'\rangle = \frac{1}{n_0}\int d\boldsymbol{c}\ \phi_m^{(\nu l)}(\alpha\boldsymbol{c})J\big[w(\alpha,c)\phi_{m'}^{[\nu'l']}(\alpha\boldsymbol{c})\big]. \tag{8}$$

For coherent scattering from structured material, the expressions are detailed in Sec. II B, while for dilute gaseous systems, all matrix elements are given explicitly in [24–28].

In the hydrodynamic regime, the space-time dependence of f is projected out through a density gradient expansion [29,30],

$$f(\boldsymbol{r},\boldsymbol{c},t) = \sum_{k=0}^{\infty} f^{(k)}(\boldsymbol{c})\odot(-\nabla)^k n(\boldsymbol{r},t), \tag{9}$$

where $f^{(k)}(\boldsymbol{c},t)$ are tensors of rank k, and $\odot$ denotes a k-fold scalar product. This expansion facilitates direct extraction of traditional transport coefficients in the hydrodynamic regime, as defined in Sec. II C. Using spherical tensors, the expansion (9) takes the form [21]

$$F_\alpha(\nu l m;\boldsymbol{r},t) = \sum_{s=0}^{2}\sum_{\lambda=0}^{s} F(\nu l m|s\lambda)G_m^{(s\lambda)}n(\boldsymbol{r},t), \tag{10}$$

where $G_m^{(s\lambda)}$ is the irreducible gradient tensor operator [21]. By substituting (10) into (7), and equating coefficients of $G_m^{(s\lambda)}n(\boldsymbol{r},t)$, we obtain the following hierarchy of kinetic equations:

$$\sum_{\nu'=0}^{\infty}\sum_{l'=0}^{\infty}\left[n_o J^{l}_{\nu\nu'}(\alpha)\delta_{ll'} - R_a\delta_{\nu\nu'}\delta_{ll'} + i\frac{qE}{m}\alpha(l'm10|lm)\langle\nu l||K^{[1]}||\nu' l'\rangle - n_0 J^{0}_{0\nu'}(\alpha)F_\alpha(\nu l0|00)(1-\delta_{s0}\delta_{\lambda 0})\delta_{l'0}\delta_{m0}\right]$$
$$\times F_\alpha(\nu' l' m|s\lambda) = \bar{X}(\nu l m|s\lambda;\alpha), \quad (\nu,l) = 0,1,2,\ldots,\infty, \quad |m| \leqslant \min\{l,\lambda\}, \quad s+\lambda = \text{even}, \tag{11}$$

where R_a is the net loss rate of charged particles and is defined in (34) below. The right-hand-side vectors for the required members of the hierarchy are given by (I.16), (I.18), and (I.20). The lowest member of the hierarchy is an eigenvalue equation, and its solution is discussed in Sec. II D. The reduced matrix elements of the velocity derivative, $\langle\nu l||K^{[1]}||\nu' l'\rangle$, are given by (I.12a). The reduced matrix elements of the collision operator have the form $\langle\nu l m||J||\nu' l' m'\rangle = J^{l}_{\nu\nu'}(\alpha)\delta_{ll'}\delta_{mm'}$ due to the scalar nature of the operator, and the evaluation of the elements is detailed in the following section.

B. Collision operators for structured matter and matrix elements in a multiterm representation

The collision operator in (1) describes the rate of change of f due to interactions with the background material. For structured media, the collision operator must account for the various scattering processes available, including coherent elastic scattering, incoherent inelastic scattering, *Ps* formation, etc., as shown in (2). In what follows, we isolate the coherent and incoherent effects and detail collision operators and associated matrix elements for each interaction process type.

1. *Coherent elastic scattering in a structured media*

The most general view of charged-particle interactions with the medium is the scattering of a wave representing the charged particle by the medium as a whole. At its simplest level, using a physical optics analogy, one can visualize this as the interference of waves diffracted from each of the constituent molecules in the materials over the domain corresponding to the range of the pair correlation function. The interference effects arising from coherent scattering processes can significantly affect the charged-particle transport within the media. These effects become important when the de Broglie wavelength of the charged particle is comparable with the average intermolecular spacing $\sim n_0^{-1/3}$. For interparticle spacings much greater than the de Broglie wavelength of the charged particle (the dilute gas-phase limit), the wave properties are suppressed and the single particle scattering regime then follows—pursuing the optics analogy, the geometric optics picture holds in this limit. This provides us with a benchmark for the coherent collision operator (and matrix elements) in this dilute gas-phase limit for which the collision operators are well known.

The matrix elements of the collision operator (omitting the space-time dependence for clarity) are related to the time rate of change of a Burnett function $\phi^{(\nu l)}_m(\alpha\boldsymbol{c})$ due to collisions via

$$\left[\frac{\partial\phi^{(\nu l)}_m(\alpha\boldsymbol{c})}{\partial t}\right]_{\text{coll}} = \int d\boldsymbol{c}\;\phi^{(\nu l)}_m(\alpha\boldsymbol{c})J[f(\boldsymbol{c})]$$
$$= n_0\sum_{\nu' l' m'}\langle\nu l m||J||\nu' l' m'\rangle F(\nu' l' m'). \tag{12}$$

From the definition of the double differential cross section $d^2\sigma/d\hat{\boldsymbol{k}}'d\omega'$, one can build up an expression for the rate of the Burnett function $\phi^{(\nu l)}_m(\alpha\boldsymbol{c})$ due to collisions:

$$\left[\frac{\partial\phi^{(\nu l)}_m(\alpha\boldsymbol{c})}{\partial t}\right]_{\text{coll}} = n_0\int d\boldsymbol{c}\;cf(\boldsymbol{c})\int_0^\infty d\omega'$$
$$\times\int_{\hat{\boldsymbol{k}}'} d\hat{\boldsymbol{k}}'\left[\phi^{(\nu l)}_m(\alpha\boldsymbol{c}) - \phi^{(\nu l)}_m(\alpha\boldsymbol{c}')\right]\frac{d^2\sigma}{d\hat{\boldsymbol{k}}'d\omega'},$$

where ω' and $\boldsymbol{k}'$, respectively, denote the angular frequency and wave number of the charged-particle wave after the interaction with the material. The double differential cross section can be expressed in term of the single particle differential cross section $\sigma_{\text{lab}}(|\Delta\boldsymbol{k}|,\hat{\boldsymbol{k}}')$ and the dynamic structure $S(\Delta\boldsymbol{k},\Delta\omega)$ [31],

$$\frac{d^2\sigma}{d\hat{\boldsymbol{k}}'d\omega'} = n_0\sigma_{\text{lab}}(|\Delta\boldsymbol{k}|,\hat{\boldsymbol{k}}')S(\Delta\boldsymbol{k},\Delta\omega), \tag{13}$$

where $\Delta\boldsymbol{k} = \boldsymbol{k} - \boldsymbol{k}'$ is the change in the wave vector ($\boldsymbol{p} = m\boldsymbol{c} = \hbar\boldsymbol{k}$) and $\Delta\omega = \omega - \omega'$ is the change in energy ($\epsilon = \hbar\omega = \hbar^2k^2/2m$ for free particles) due to the interaction with the medium. Undashed and dashed quantities refer to their properties before and after interactions, respectively. In what follows, we have set $\hbar = 1$ for convenience. All expressions are evaluated in the laboratory frame. This contrasts with the single molecule scattering case, where collisions are carried out in the center of mass frame; for interactions with many particles simultaneously, this is not possible. The dynamic structure factor must satisfy the first three sum rules,

$$\int_{-\infty}^{\infty} dQ\;S(\boldsymbol{K},Q) = S(\boldsymbol{K}), \tag{14}$$

$$\int_{-\infty}^{\infty} dQ\;QS(\boldsymbol{K},Q) = \frac{K^2}{2m_0}, \tag{15}$$

$$\int_{-\infty}^{\infty} dQ\;Q^2S(\boldsymbol{K},Q) \approx 2kT_0\frac{K^2}{2m_0}, \tag{16}$$

where T_0 is the temperature of the medium and m_0 is the mass of the constituent atoms and molecules. These sum rules require the independence of $\boldsymbol{K}$ and Q. The dynamic structure factor is the space and time Fourier transform of the Van Hove time-dependent, generalized, pair-distribution function, while the static structure factor $S(\boldsymbol{K})$ is the Fourier transform of the radial pair-distribution function [31]. Pursuing the physical optics analogy with a multislit experiment again, the overall pattern derives from a superposition of the interference patterns of the combined slits (scattering centers) with the diffraction pattern of each slit (single particle scattering). The former is governed by the static structure factor, while the latter is governed by the scattering cross section. Furthermore, the diffraction patterns are Doppler shifted depending on the relative velocity of the atom or molecules and the charged particles, and this manifests itself in the appearance of the medium temperature in the sum rules.

From the definition of (13), one can construct the following expression for the rate of change of $\phi_m^{[\nu l]}(\alpha\boldsymbol{c})$ due to interactions with the medium per unit volume:

$$\left[\frac{\partial\phi_m^{(\nu l)}(\alpha\boldsymbol{c})}{\partial t}\right]_{\mathrm{coll}} = n_0\int d\boldsymbol{c}\; cf(\boldsymbol{c})\int_{-\infty}^{\infty} d(\Delta\omega) \times \int_{\hat{\boldsymbol{k}}} d\Omega_{\boldsymbol{k}'}\left[\phi_m^{(\nu l)}(\alpha\boldsymbol{c}) - \phi_m^{(\nu l)}(\alpha\boldsymbol{c}')\right] \times \sigma_{\mathrm{lab}}(|\Delta\boldsymbol{k}|,\hat{\boldsymbol{k}}')S(\Delta\boldsymbol{k},\Delta\omega). \tag{17}$$

To zero order in $\Delta\omega/\frac{1}{2}mc^2$, the above expression is nonzero for all $l \geqslant 1$, and this level of approximation is sufficient. For $l = 0$, however, the expression is identically zero and a first-order correction is required. Given the dependence of $\Delta\boldsymbol{k}$ and $\Delta\omega$, we cannot implement the sum rules to evaluate the expressions involving $S(\Delta\boldsymbol{k},\Delta\omega)$. To enforce independence, we expand about zero energy exchange, with an associated momentum exchange $\Delta\boldsymbol{k}_0$, where $\boldsymbol{k}$ is merely rotated through a scattering angle χ during an interaction without a change in its magnitude, and hence

$$\Delta\boldsymbol{k} = \boldsymbol{k} - \boldsymbol{k}' = \Delta\boldsymbol{k}_0 + (k - k')\hat{\boldsymbol{k}}'. \tag{18}$$

We note that the following approximations exist in the limit of small $\Delta\omega/\frac{1}{2}mc^2$:

$$\sigma_{\mathrm{lab}}(|\Delta\boldsymbol{k}|,\hat{\boldsymbol{k}}') \approx \sigma(c,\chi) - \frac{c}{4}\left(\frac{\Delta\omega}{\frac{1}{2}mc^2}\right)\frac{\partial}{\partial c}\sigma(c,\chi), \tag{19}$$

$$S(\Delta\mathbf{k},\Delta\omega) \approx S(\Delta\boldsymbol{k}_0,\Delta\omega) + \frac{mc}{2}\left(\frac{\Delta\omega}{\frac{1}{2}mc^2}\right)\widehat{\boldsymbol{k}'} \cdot\left[\frac{\partial}{\partial\boldsymbol{K}}\,S(\boldsymbol{K},\Delta\omega)\right]_{\boldsymbol{K}=\Delta\boldsymbol{k}_0}, \tag{20}$$

where (19) follows from [31].

We consider initially the case for $l = 0$,

$$\left[\frac{\partial\phi_0^{(\nu 0)}(\alpha\boldsymbol{c})}{\partial t}\right]_{\mathrm{coll}} = n_0\,\frac{1}{\sqrt{4\pi}}\int d\boldsymbol{c}\; c\; f(\boldsymbol{c})\int_{\hat{\boldsymbol{\Omega}}_{k'}} d\hat{\boldsymbol{\Omega}}_{k'} \times [R_{\nu 0}(\alpha c) - R_{\nu 0}(\alpha c')]\sigma_{\mathrm{lab}}(|\Delta\boldsymbol{k}|,\hat{\boldsymbol{k}}')S(\Delta\boldsymbol{k},\Delta\omega).$$

Using expansions (19) and (20) along with a Taylor series expansion of $R_{\nu 0}(\alpha c')$, enforcing the sum rules (14)–(16), it follows that to first order in $\Delta\omega/\frac{1}{2}mc^2$, this expression reduces to

$$\left[\frac{\partial\phi_0^{(\nu 0)}(\alpha\boldsymbol{c})}{\partial t}\right]_{\mathrm{coll}} = n_0\,\frac{1}{\sqrt{4\pi}}\int d\boldsymbol{c}\; c\; f(\boldsymbol{c})\frac{m}{m_0 c^2} \times\left\{c^4\sigma_m(c)R'_{\nu 0}(\alpha c) - \frac{kT_0}{m}\frac{\partial}{\partial c}[c^3\sigma_m R'_{\nu 0}(\alpha c)]\right\}.$$

This expression can be shown to be equivalent to the traditional Davydov collision operator used to describe elastic collisions in gaseous systems.

For $l \geqslant 1$, a zeroth order truncation in $\Delta\omega/\frac{1}{2}mc^2$ in (17) is sufficient. In this limit, we can perform the integration over $\Delta\omega$, and it follows that

$$\left[\frac{\partial\phi_m^{(\nu l)}(\alpha\boldsymbol{c})}{\partial t}\right]_{\mathrm{coll}} = n_0\,2\pi\int d\boldsymbol{c}\; c\; f(\boldsymbol{c})\int_{-1}^{1} d(\cos\chi)R_{\nu l}(\alpha c) \times\left[Y_m^{[l]}(\hat{\boldsymbol{c}}) - Y_m^{[l]}(\hat{\boldsymbol{c}}')\right]\Sigma(c,\chi), \tag{21}$$

where

$$\Sigma(c,\chi) = \sigma(c,\chi)\;S\left(\frac{2mc}{\hbar}\sin\frac{\chi}{2}\right) \tag{22}$$

is an effective differential cross section for higher order equations where $l \geqslant 1$. Note that, at this point, we have assumed that the medium is isotropic and hence $S(\Delta\boldsymbol{k}_0) = S(|\Delta\boldsymbol{k}_0|) = S(\frac{2mc}{\hbar}\sin\frac{\chi}{2})$. If we represent $\Sigma(c,\chi)$ through an expansion in terms of Legendre polynomials,

$$\Sigma(c,\chi) = \sum_{\lambda=0}^{\infty}\frac{2\lambda+1}{2}\Sigma_\lambda(c)P_\lambda(\cos\chi), \tag{23}$$

then one can make connection with the previous calculations of the collision matrix elements for dilute gaseous systems. The effective partial cross sections $\Sigma_l(c)$ are defined by

$$\Sigma_l(c) = 2\pi\int_{-1}^{1}\Sigma(c,\chi)P_l(\cos\chi)d(\cos\chi) = \frac{1}{4\pi}\sum_{\lambda'\lambda''}\frac{(2\lambda'+1)(2\lambda''+1)}{2l+1}(\lambda' 0\lambda'' 0|l0)^2\sigma_{\lambda'}(c)s_{\lambda''}(c),$$

where

$$\sigma_l(c) = 2\pi\int_{-1}^{1}\sigma(c,\chi)P_l(\cos\chi)d(\cos\chi) \tag{24}$$

and

$$s_l(c) = \frac{1}{2}\int_{-1}^{1}S\left[\frac{2mc}{\hbar}\sin\left(\frac{\chi}{2}\right)\right]P_l(\cos\chi)d(\cos\chi). \tag{25}$$

This relationship is valid for anisotropic scattering processes. For dilute gases, $S(\Delta K) = 1$, and it follows that $s_l(c) = \delta_{l0}$ and the expressions reduce to the dilute gaseous form in the equivalent mass ratio limit [24]. We should highlight that for isotropic scattering, in the two-term approximation, the structure-modified momentum transfer cross section $\Sigma_m = \Sigma_0 - \Sigma_1$ only samples $s_0 - s_1$ or the $(1 - \cos\chi)$ moment of the static structure factor S [17]. In this multiterm theory, we are able to sample higher order moments of S.

Finally, to evaluate the collision matrix elements, we expand the velocity distribution function using (5), and using the orthonormality relations, it then follows that

$$\langle\nu lm||J||\nu' l' m'\rangle = V_{\nu\nu'}^{l}\delta_{ll'}\delta_{mm'}, \tag{26}$$

where

$$V_{\nu\nu'}^{0} = \frac{m}{m_0}\int_0^{\infty} w(\alpha,c)R_{\nu' 0}(\alpha c)\left\{[\sigma_0(c) - \sigma_l(c)]\left(c^2 R'_{\nu 0}(\alpha c) - \frac{kT_0}{m}[3R'_{\nu 0}(\alpha c) + cR''_{\nu 0}(\alpha c)]\right) - [\sigma_0'(c) - \sigma_l'(c)]cR'_{\nu 0}(\alpha c)\right\}c^2 dc, \tag{27}$$

$$V^{l}_{\nu\nu'} = \int_0^\infty w(\alpha,c)R_{\nu' l}(\alpha c)[\Sigma_0(c) - \Sigma_l(c)]R_{\nu l}(\alpha c)c^3 dc, \tag{28}$$

in which the dashes refer to speed derivatives and $V^{l}_{\nu\nu'}$ are interaction integrals [24,25] generalized to account for the effects of coherent scattering from structured media. One can establish the connection with the matrix elements in the dilute gas case limit [24,25].

2. *Incoherent scattering and particle loss processes*

For inelastic processes, energy is transferred on a localized site during scattering. Scattering is hence incoherent and interference effects cannot manifest themselves. We use the semiclassical extension of the Boltzmann collision operator [32] to represent such processes. Processes such as attachment, annihilation, and *Ps* formation from a kinetic theory viewpoint are simple particle loss processes, and hence the collision operators representing such processes are just the direct scattering part of the original Boltzmann collision operator [33]. Consequently, the structure of the material does not play a role in these interaction processes. Expressions for the collision matrix elements for the incoherent inelastic scattering and loss processes (e.g., attachment, *Ps* formation) are detailed in [24,25].

C. Transport coefficients and properties

Experimental investigations of transport behavior are generally made by sampling charged-particle currents or densities, $n(\boldsymbol{r},t) = \int f(\boldsymbol{r},\boldsymbol{c},t)d\boldsymbol{c}$. The connection between experiment and theory is made through the equation of continuity

$$\frac{\partial n(\boldsymbol{r},t)}{\partial t} + \nabla \cdot \boldsymbol{\Gamma}(\boldsymbol{r},t) = S(\boldsymbol{r},t), \tag{29}$$

where $\boldsymbol{\Gamma}(\boldsymbol{r},t) = n\langle \boldsymbol{c}\rangle$ is the charged-particle flux and $S(\boldsymbol{r},t)$ represents the production rate per unit volume, per unit time, arising from nonconservative collisional processes, such as *Ps* formation or annihilation for positron systems, or ionization and attachment processes for electrons. Assuming the functional relationship (9), the flux $\boldsymbol{\Gamma}(\boldsymbol{r},t)$ and source term $\boldsymbol{S}(\boldsymbol{r},t)$ in (29) are expanded as follows:

$$\boldsymbol{\Gamma}(\boldsymbol{r},t) = \boldsymbol{W}_F n(\boldsymbol{r},t) - \mathbf{D}_F \cdot \nabla n(\boldsymbol{r},t) + \cdots \tag{30}$$

$$\boldsymbol{S}(\boldsymbol{r},t) = S^{(0)} - \boldsymbol{S}^{(1)} \odot \nabla n(\boldsymbol{r},t) + \mathbf{S}^{(2)} \odot \nabla\nabla n(\boldsymbol{r},t) \ + \cdots, \tag{31}$$

where $\boldsymbol{W}_F$ is the flux drift velocity and $\mathbf{D}_F$ is the flux diffusion tensor. Expansion (30) is a generalization of the traditional Fick's law to higher order. Substitution of expansions (30) and (31) into the continuity Eq. (29) yields the generalized diffusion equation

$$\frac{\partial n}{\partial t} + \boldsymbol{W} \cdot \nabla n - \mathbf{D} : \nabla\nabla n + \cdots = -R_a n \ , \tag{32}$$

where $R_a = -S^{(0)}$ is the loss rate, and we define the bulk transport coefficients as

$$\boldsymbol{W} = \boldsymbol{W}_F + S^{(1)}; \qquad \mathbf{D} = \mathbf{D}_F + \mathbf{S}^{(2)}. \tag{33}$$

Swarm experiments are generally analyzed on the basis of the diffusion equation and hence it is the bulk coefficients, not the flux, that are generally determined in swarm experiments. We note, however, that it is often the flux coefficients that are required in fluid models of these systems [34]. The transport coefficients of interest in the present study are related to the calculated moments via

$$R_a = n_0 \sum_{\nu'=0}^{\infty} J^0_{0\nu'}(\alpha)F_\alpha(\nu'00|00), \tag{34}$$

$$W = \frac{i}{\alpha}F_\alpha(010|00) - in_0 \sum_{\nu'=1}^{\infty} J^0_{0\nu'}(\alpha)F_\alpha(\nu'00|11), \tag{35}$$

$$D_L = -\frac{1}{\alpha}F_\alpha(010|11) - n_0 \sum_{\nu'=1}^{\infty} J^0_{0\nu'}(\alpha) \times [F_\alpha(\nu'00|20) - \sqrt{2}F_\alpha(\nu'00|22)], \tag{36}$$

$$D_T = -\frac{1}{\alpha}F_\alpha(011|11) - n_0 \sum_{\nu'=1}^{\infty} J^0_{0\nu'}(\alpha) \times \left[F_\alpha(\nu'00|20) + \frac{1}{\sqrt{2}}F_\alpha(\nu'00|22)\right]. \tag{37}$$

We reemphasize here that there are two distinct "sets" of cross sections: bulk and flux [34–36]. The drift velocity and diffusion coefficients defined above are bulk coefficients. The components involving summations constitute the explicit nonconservative components of the transport coefficients, while the remainder constitute the flux contribution. Using expansion (9), we can represent the spatial dependence of the average energy in a density gradient expansion,

$$\epsilon(\boldsymbol{r},t) = \varepsilon + \boldsymbol{\gamma} \cdot \frac{\nabla n}{n} + \cdots, \tag{38}$$

where ε and γ are the spatially homogeneous mean energy and gradient energy parameter [37], respectively, and are calculated from the moments according to

$$\varepsilon = \frac{3}{2}kT_b\left[1 - \sqrt{\frac{2}{3}}F_\alpha(100|00)\right], \tag{39}$$

$$\boldsymbol{\gamma} = \frac{3}{2}kT_b\left\{\sqrt{\frac{2}{3}}\mathrm{Im}[F_\alpha(100|11)]\right\}, \tag{40}$$

where $\mathrm{Im}\{\cdot\}$ denotes the imaginary part of the moment. The expansion (38) serves to facilitate our discussions of phenomena related to the spatial variation of the average energy through the swarm, including anisotropic diffusion and the explicit effects of *Ps* formation.

D. Numerical solution of the hierarchy

The solution of (11) for the transport properties above requires the solution of five members of the hierarchy determined by $(s,\lambda,m) = (0,0,0),(1,1,0),(1,1,1),(2,0,0),(2,2,0)$. The order of solution of members (defined by the m index) within a given level of the hierarchy [defined by $(s,\ \lambda)$] is arbitrary. The spatially homogeneous member of the hierarchy $(s,\lambda,m) = (0,0,0)$ is an eigenvalue problem and, together with (34), constitute a system of coupled nonlinear equations, which are solved iteratively for the moments $F_\alpha(\nu l m|00)$ and the loss rate R_a. The remaining members of the hierarchy can be solved via direct numerical inversion. The coefficient matrix exhibits a tridiagonal block structure, with off-diagonal blocks sparse. We employ a sparse matrix routine to exploit this property. The numerical solution of (11) requires truncation of the ν and l summations to manageably finite values $\nu_{\max}$ and $l_{\max}$, respectively. These values are incremented independently until a specified accuracy criteria is satisfied on the transport properties. The required values of $l_{\max}$ and $\nu_{\max}$ represent, respectively, the deviation of the velocity distribution from spherical symmetry and the deviation of the speed distribution from a Maxwellian distribution at T_b. For details, the reader is referred to [25].

III. RESULTS AND DISCUSSION

A. Benchmark model

1. The model: Free electrons in a dense gas of hard spheres

To elucidate the essential physics of the transport of light particles in a dense structured media, we implement the simplest model of such a system. The structure of the system is described by the Percus-Yevick structure function (with the Verlet-Weis correction) [38] representing a systems of hard-spherical particles. The key parameter is the volume fraction Φ describing the ratio of the volume of spheres to the total volume, and is a measure of the packing of the spherical particles. The physical dimensions of the constituent particles are such that they have a cross-sectional area of 6 Å^2. We consider a charged-particle–neutral-particle interaction cross section that is governed by an isotropic constant cross section of the same amplitude. We assume the temperature of the material is 0 K, the mass of the constituent neutral particles is 4 amu, and the charged particles are electrons. All quantities are analytic so that this model can provide a benchmark for further modeling in this field.

The static structure functions for the Percus-Yevick model corresponding to various volume fractions are displayed in Fig. 1. The structure-modified momentum transfer cross sections associated with the various volume fractions, as displayed in Fig. 2, decrease with increasing volume fraction. In Fig. 3, we display the low-order modified partial cross-section combinations ($l \leqslant 4$) appearing in the multiterm theory for a fixed volume fraction. Physically, one expects that as the energy increases, and hence de Broglie wavelength decreases, the effects of coherent scattering are reduced and the structure-modified cross sections approach the dilute gas-phase cross sections. This is reflected in Figs. 2 and 3.

2. Spatially homogeneous transport properties

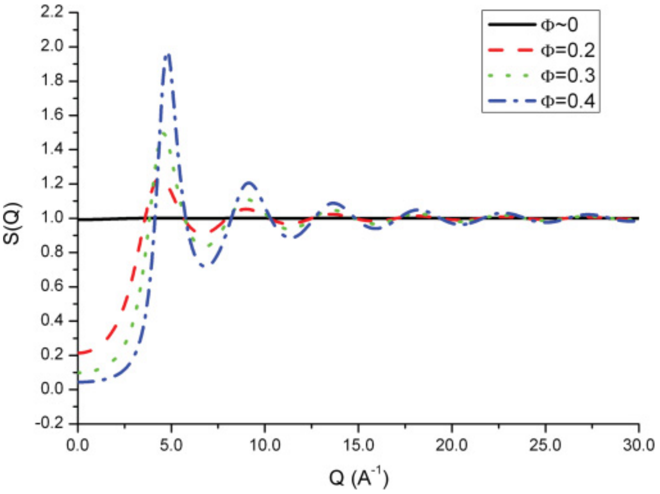

FIG. 1. (Color online) The variation of the static structure factor with momentum exchange Q for the modified Percus-Yevick model at various volume fractions.

In Fig. 4, we display the variation of the mean energy of the swarm as a function of the applied reduced electric field E/n_0, where n_0 is the number density of the scatterers (1 townsend = 1 Td = 10^{21} V m^2). The results are compared for various volume fractions Φ and in the limit of the dilute gas phase $\Phi \approx 0$. In the dilute gas case, the mean energy exhibits the expected linear dependence upon the field. In the low-field regime, the mean energy increases with increasing volume fraction. The reduction in the structure-modified momentum transfer cross section with increasing volume fraction for low energies reduces the randomizing nature of collisions and allows the electric field to efficiently pump energy into the swarm. The coalescence of the various profiles at high fields and hence energies is a reflection of the decrease in the de Broglie wavelength and the consequent suppression of the coherent scattering effects.

In Fig. 5, the impact of volume fraction on the field dependence of the drift velocity is displayed. At low fields, the impact of the reduction in the randomizing nature of the interactions with Φ is evidenced by the increased directed motion and hence drift velocity. Importantly, we notice, for volume fractions above a critical value, the existence of negative differential conductivity (NDC), i.e., the reduction in the drift velocity with increasing fields. This form of negative differential conductivity arises purely as a consequence of the coherent scattering from a structured material, and is referred to as structure-induced NDC [14]. This phenomenon has also been observed in other electron calculations [17]. In contrast to other forms of NDC for electron transport in dilute

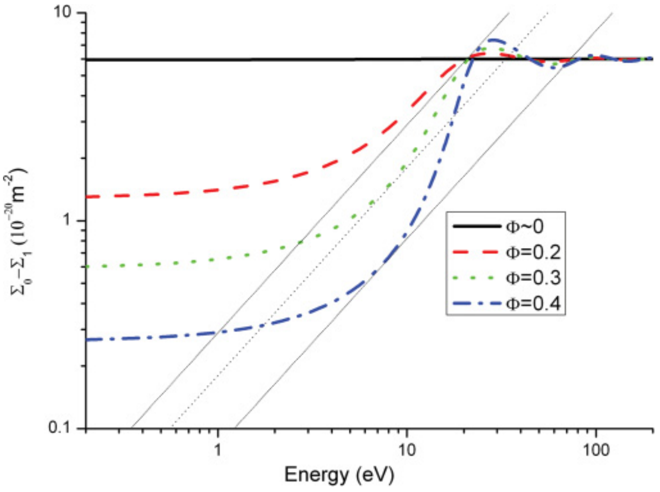

FIG. 2. (Color online) The energy variation of the structure-modified momentum transfer cross section for the modified Percus-Yevick model for various volume fractions.

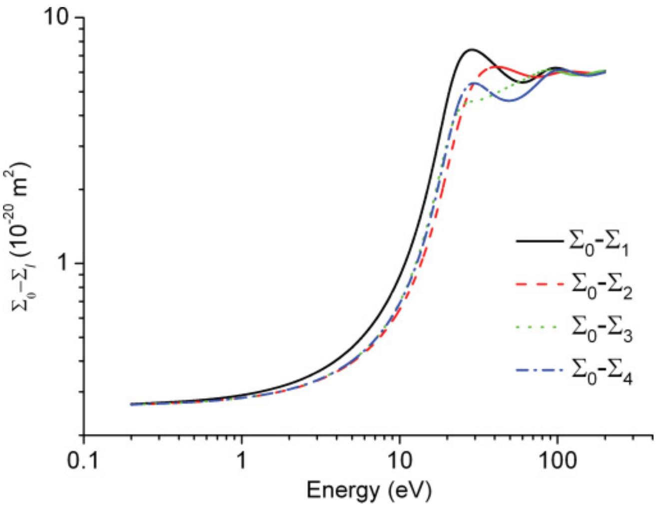

FIG. 3. (Color online) The energy variation of low-order, structure-modified, partial cross-section combinations for the modified Percus-Yevick model with a volume fraction $\Phi = 0.4$.

gases [39–41], this form does not require inelastic scattering processes or nonconservative processes such as annihilation and attachment [12,13]. In [14], the following condition for the existence of structure-induced NDC was presented:

$$\frac{d\ln(s_0 - s_1)}{d\ln\varepsilon} > 1\,. \tag{41}$$

In Fig. 2, we have included the criteria lines for emphasis and we observe that the condition is consistent with the results in Fig. 5. For volume fractions above 0.2, this criterion is met for a range of fields where mean energy falls in this window.

3. Spatially inhomogeneous transport properties

The phenomenon of anisotropic diffusion is well known for charged particles of all masses in dilute gaseous systems. For the light particles and the hard-sphere model under consideration here, the ratio of the longitudinal to transverse diffusion coefficients is approximately 0.5 [42], and this benchmark is met in Fig. 6 for the $\Phi = 0$ case. This figure also highlights the impact of coherent scattering effects on the nature of diffusion. For low fields, we observe that diffusion is enhanced by nearly two orders of magnitude with increasing Φ. This is due to the implicit enhanced thermal effects and the explicit effects of a reduction in the momentum transfer cross section. Interestingly, the ratio remains at 0.5 in this field range. In the energy regime, the effective momentum transfer cross section is approximately constant with the energy for all volume fractions, and it follows that the D_L/D_T ratio is fixed at approximately 0.5. For the volume fractions displayed, all diffusion coefficients have a window of field strengths where they are decreasing with increasing field. This is a reflection of the regime where the momentum transfer collision frequency increases rapidly with energy. The decrease is particularly significant for the longitudinal component where it can fall by as much as an order of magnitude. There are two explicit effects which contribute to this: (i) the thermal effects, which are essentially manifest in the transverse diffusion coefficient, and (ii) the differential velocity effect [37]. The differential velocity effect is a combination of a collision frequency, which varies with energy, and an average energy, which varies through the swarm as detailed by the parameter γ [37]. The variation of γ with the field is displayed in Fig. 7. Although the gradient energy parameter γ falls slightly with the field in this regime, this differential velocity effect is enhanced by virtue of the rapidly increasing momentum transfer collision frequency in this regime. The large reduction in the longitudinal component with the field in this regime then follows.

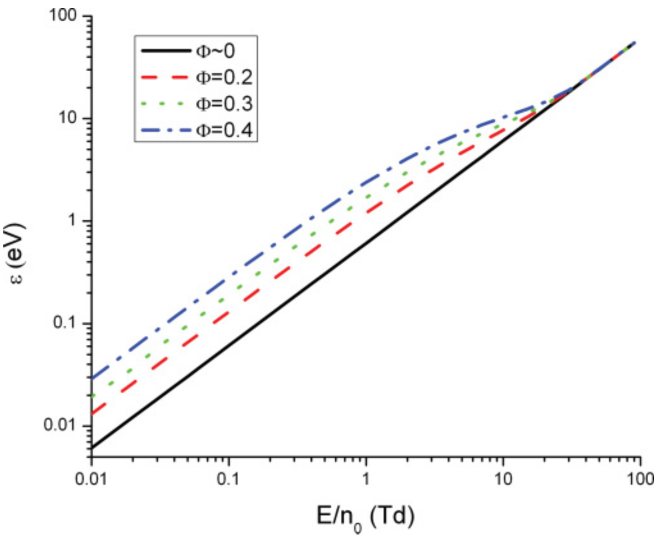

FIG. 4. (Color online) Variation of the mean energy with reduced electric field for various volume fractions Φ for a dense gas of hard spheres.

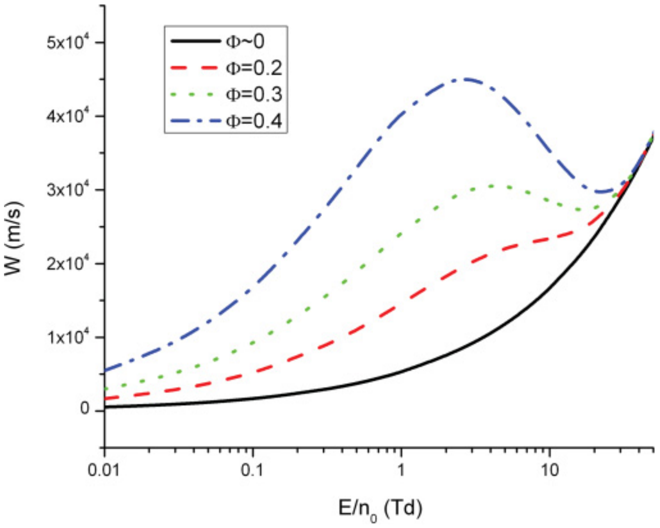

FIG. 5. (Color online) Variation of the drift velocity with reduced electric field for various volume fractions Φ for a dense gas of hard spheres.

4. The accuracy of the two-term approximation

In the dilute gaseous case for the hard-sphere model, the two-term approximation is generally accurate to within 0.5%

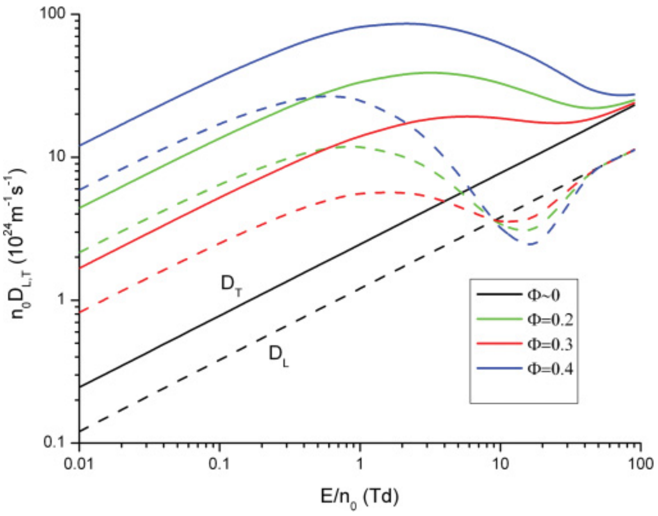

FIG. 6. (Color online) Variation of the charged-particle diffusion coefficients with reduced electric field for various volume fractions Φ for a dense gas of hard spheres (solid line is n_0D_T; dashed line is n_0D_L).

or better for all transport coefficients. In Fig. 8, we present the accuracy of the two-term approximation for the various transport coefficients as a function of the applied field. As detailed in Sec. II, by including more terms in the expansion (3), we sample more moments of the static structure factor s_l and hence include more information about the material properties. The importance of sampling higher order moments, even for this simple model, is highlighted in Fig. 8.

B. Transport of spatially inhomogeneous positrons in liquid argon

In this section, we extend results from our previous paper [14] to now consider spatially inhomogeneous transport coefficients. We utilize these spatially inhomogeneous transport coefficients to discuss the phenomenon of NDC arising from the explicit influence of *Ps* formation [12–14]. Details of the cross sections, structure factors, and the structure-modified cross sections are given in [14].

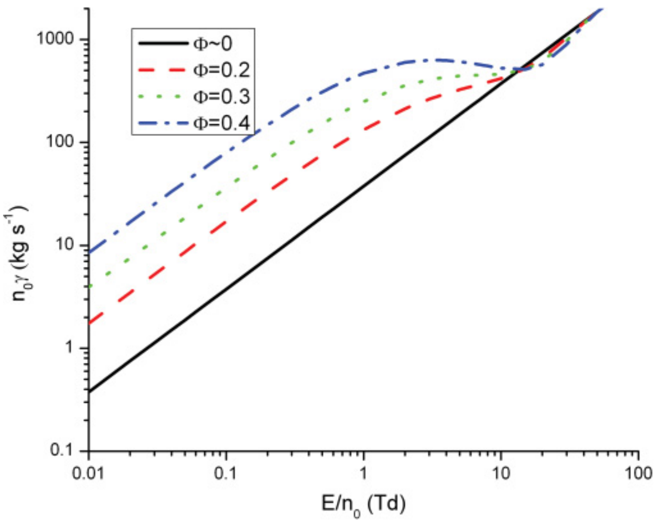

FIG. 7. (Color online) Variation of the charged-particle gradient energy parameter γ with reduced electric field for various volume fractions Φ for a dense gas of hard spheres.

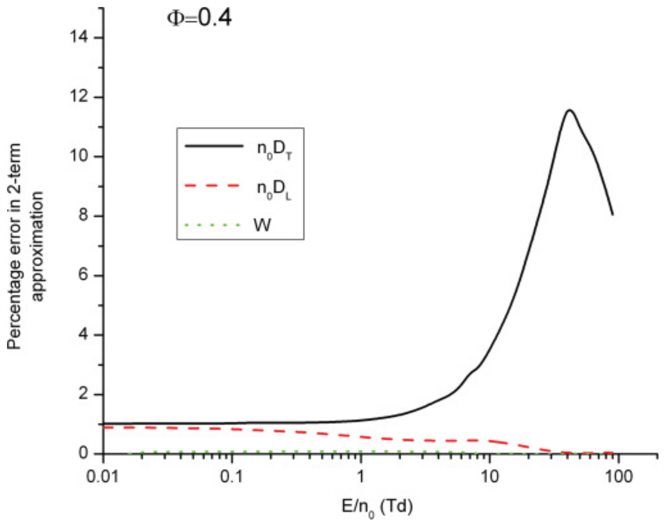

FIG. 8. (Color online) Accuracy of the two-term approximation for the various charged-particle transport properties for a dense gas of hard spheres with volume fraction $\Phi = 0.4$.

In Fig. 9, we display the flux diffusion coefficients for positrons in liquid argon. Much of the phenomenology observed for the model dense gas system in Sec. III A 3 carries over to the liquid argon system. In the low-field regime, where coherent scattering effects are important, we observe distinctly different behaviors in the transport properties as compared to the dilute gas-phase case. The thermal values (i.e., low field) of the flux diffusion coefficients of positrons in liquid argon are at least an order of magnitude greater for a liquid than for a dilute gas. The origin of this behavior was discussed in Sec. III A 3. In the high-field (high-energy) limit, the positron de Broglie wavelengths decrease, coherent scattering becomes less important, and the liquid-phase and dilute gas-phase results converge as in the model case. The region of rapid increase in both components of the diffusion tensor reflects a rapidly falling effective cross section in this

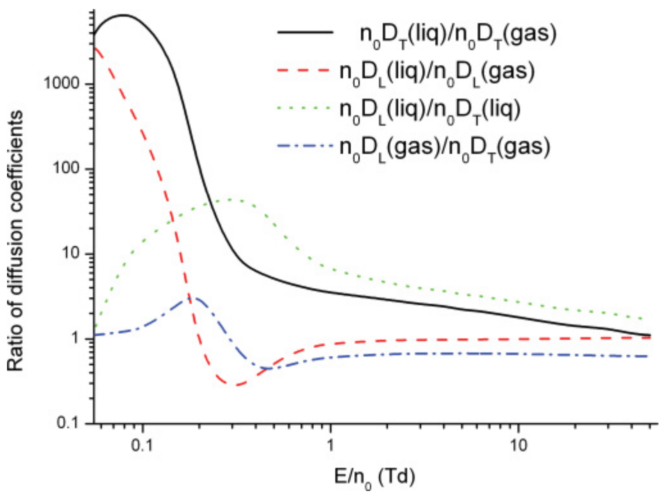

FIG. 9. (Color online) The flux diffusion coefficients of positrons in liquid and dilute gaseous Ar at 85 K as a function of E/n_0.

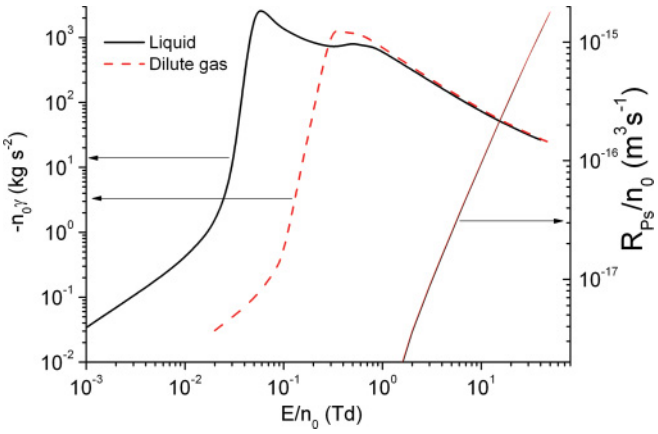

FIG. 10. (Color online) The positronium formation rate and gradient energy parameter for positrons in liquid and dilute gaseous Ar at 85 K as a function of E/n_0.

energy regime. The anisotropic nature of diffusion for positron in liquids, as reflected in the disparity between the longitudinal and transverse diffusion coefficients, is significantly increased over the dilute gas phase. From Fig. 9, we observe that the difference can be up to almost two orders of magnitude for liquids, in contrast to a factor of 2 to 3 for the dilute gas phase. This is a manifestation of the enhanced spatial variation of the average energy (γ) (see Fig. 10) combined with a rapidly varying effective collision frequency in this field domain.

The gradient energy parameter also presents a convenient way to discuss the phenomenon of positronium (Ps)-induced NDC that was originally observed and discussed for gases [12,13] and, recently, in the context of liquids [14]. To understand this phenomenon, we must first identify that the bulk drift velocity is the time rate of change of the center of mass of the swarm of positrons. It is composed of the flux drift velocity (mean velocity of electrons) plus a contribution brought about by the nonsymmetric loss of positrons to the swarm to Ps formation ($S^{(1)}$). Since on average the positrons at the front of the swarm are more energetic than those at the trailing edge, as reflected by the transport property γ (see Fig. 10), there is a preferential loss of positrons to Ps formation at the front of the swarm relative to the back. This results in a shift in the center of mass of the swarm in the opposite direction to the field force direction. Consequently, the bulk drift velocity is less than the flux drift velocity. The strength of the Ps formation processes in the field in the range 0.5–15 Td (see Fig. 10), combined with a sufficiently strong variation in the average energy (i.e., the high γ shown in Fig. 10), is such that NDC results in this field region (see Fig. 3 of Ref. [14]). One of the key questions that remains is why NDC terminates for higher fields given the monotonic increase in the Ps formation rates with increasing field. The answer lies in the falloff of γ with increasing field. At higher fields, there is no longer sufficient nonsymmetric spatial variation in the average energy through the swarm to generate the required preferential loss of positrons from the front of the swarm for the generation of NDC.

IV. CONCLUDING REMARKS

In this work, we have presented a systematic treatment of nonequilibrium charged-particle transport in structure soft condensed media, generalizing the Boltzmann kinetic equation originally proposed by Cohen and Lekner [15]. We have explicitly included the effects of coherent and incoherent scattering as well as particle loss processes. Transport properties are determined by a combination of the static structure factor and the single particle scattering cross sections. We have presented details of a multiterm solution of the structure-modified kinetic equation, which overcomes the accuracy limitations associated with a two-term approximation of Cohen and Lekner [15] generally applied to electron and positron transport in liquids and dense gases. In addition, we have formulated and implemented a consistent nonperturbative treatment of loss rates, avoiding the limitations of previous perturbative schemes. The theory and associated codes have been applied to a model Percus-Yevick system and then to positrons in liquid argon. Phenomena have been found that arise explicitly from the coherent nature of scattering and become manifest particularly at low fields, including structure-induced negative differential conductivity and structure-induced anisotropic diffusion. In the limiting case of high fields (high energies and smaller de Broglie wavelengths), the structure effects are negligible and the traditional dilute gas-phase kinetic equation and associated results are retained.

ACKNOWLEDGMENTS

The authors would like to acknowledge the support of the Australian Research Council and Queensland Smart Futures fund.

---

[1] B. Baibussinov, M. B. Ceolin, E. Calligarich, S. Centro, K. Cieslik, C. Farnese, A. Fava, D. Gibin, A. Guglielmi, G. Meng, F. Pietropaolo, C. Rubbia, F. Varanini, and S. Ventura, J. Instrum. **5**, P03005 (2010).

[2] N. Tessler, Y. Preezant, N. Rappaport, and Y. Roichman, Adv. Mater. **21**, 2741 (2009).

[3] Y. Zheng, J. R. Wagner, and L. Sanche, Phys. Rev. Lett. **96**, 208101 (2006).

[4] H. Nikjoo, D. Emfietzoglou, R. Watanabe, and S. Uehara, Radiat. Phys. Chem. **77**, 1270 (2008).

[5] S. R. Cherry, J. A. Sorensen, and M. E. Phelps, *Physics in Nuclear Medicine* (Saunders, Philadelphia, 2003), p. 544.

[6] H. P. D. W. Gidley and R. S. Vallery, Annu. Rev. Mater. Res. **36**, 49 (2006).

[7] S. Buckman and C. Clark, Rev. Mod. Phys. **66**, 539 (1994).

[8] M. J. Brunger and S. J. Buckman, Phys. Rep. **357**, 215 (2002).

[9] H. Hotop, M. W. Ruf, M. Allan, and I. I. Fabrikant, Adv. At. Mol. Phys. **49**, 85 (2003).

[10] C. M. Surko, G. F. Gribakin, and S. J. Buckman, J. Phys. B **38**, R57 (2005).

[11] J. P. Sullivan, C. Makochekanwa, A. Jones, P. Caradonna, and S. J. Buckman, J. Phys. B **41**, 081001 (2008).
[12] M. Suvakov, Z. L. Petrovic, J. P. Marler, S. J. Buckman, R. E. Robson, and G. Malovic, New J. Phys. **10**, 053034 (2008).
[13] A. Bankovic, Z. L. Petrovic, R. E. Robson, J. P. Marler, S. Dujko, and G. Malovic, Nucl. Instrum. Methods Phys. Res. B **267**, 350 (2009).
[14] R. D. White and R. E. Robson, Phys. Rev. Lett. **102**, 230602 (2009).
[15] M. H. Cohen and J. Lekner, Phys. Rev. **158**, 305 (1967).
[16] Y. Sakai, J. Phys. D **40**, R441 (2007).
[17] V. M. Atrazhev and E. G. Dmitriev, J. Phys. C **18**, 1205 (1985).
[18] A. F. Borghesani, IEEE Trans. Dielectr. Electr. Insul. **13**, 492 (2006).
[19] R. D. White, R. E. Robson, B. Schmidt, and M. A. Morrison, J. Phys. D **36**, 3125 (2002).
[20] I. Pepe, D. A. L. Paul, J. Steyaert, F. Gimeno-Nogues, J. Deutsch, and R. Prieels, J. Phys. B **28**, 3643 (1995).
[21] R. E. Robson and K. F. Ness, Phys. Rev. A **33**, 2068 (1986).
[22] E. A. Mason and E. W. McDaniel, *Transport Properties of Ions in Gases* (Wiley, New York, 1988).
[23] S. Chapman and T. G. Cowling, *The Mathematical Theory of Non-Uniform Gases* (Cambridge University Press, Cambridge, 1939).
[24] S. L. Lin, R. E. Robson, and E. A. Mason, J. Chem. Phys. **71**, 3483 (1979).
[25] K. F. Ness and R. E. Robson, Phys. Rev. A **34**, 2185 (1986).
[26] K. Kumar, Ann. Phys. **37**, 113 (1966).
[27] K. Kumar, J. Math. Phys. **7**, 671 (1966).
[28] K. Kumar, Aust. J. Phys. **20**, 205 (1967).
[29] K. Kumar, H. R. Skullerud, and R. E. Robson, Aust. J. Phys. **33**, 343 (1980).
[30] R. D. White, R. E. Robson, S. Dujko, P. Nicoletopoulos, and B. Li, J. Phys. D **42**, 194001 (2009).
[31] L. Van Hove, Phys. Rev. **95**, 249 (1954).
[32] C. S. Wang-Chang, G. E. Uhlenbeck, and J. De Boer, in *Studies in Statistical Mechanics*, edited by J. D. Boer and G. E. Uhlenbeck (Wiley, New York, 1964), Vol. II, p. 241.
[33] L. Boltzmann, Wein. Ber. **66**, 275 (1872).
[34] R. E. Robson, R. D. White, and Z. L. Petrović, Rev. Mod. Phys. **77**, 1303 (2005).
[35] R. Robson, Aust. J. Phys. **44**, 685 (1991).
[36] H. Tagashira, T. Taniguchi, K. Kitamori, and Y. Sakai, J. Phys. D **11**, L43 (1978).
[37] R. D. White, R. E. Robson, and K. F. Ness, Aust. J. Phys. **48**, 925 (1995).
[38] L. Verlet and J. Weis, Phys. Rev. A **5**, 939 (1972).
[39] Z. L. Petrović, R. W. Crompton, and G. N. Haddad, Aust. J. Phys. **37**, 23 (1984).
[40] R. E. Robson, Aust. J. Phys. **37**, 35 (1984).
[41] S. B. Vrhovac and Z. L. Petrović, Aust. J. Phys. **52**, 999 (1999).
[42] R. E. Robson, *Introductory Transport Theory for Charged Particles in Gases* (World Scientific, Singapore, 2006), p. 181.